Vertical Profiles of Soil Resistivity at Pampa La Bola and Llano de Chajnantor Locations

Seiichi Sakamoto
National Astronomical Observatory of Japan
Mitaka, Tokyo 181-8588, Japan

Hajime Ezawa, Toshikazu Takahashi, and Nobuyuki Yamaguchi
Nobeyama Radio Observatory
Minamimaki, Minamisaku, Nagano 384-1305, Japan

October 12, 2000

Abstract

We report results of resistivity sounding of eight locations in the Cerro Chascón science preserve area. The soil resistivity near the surface was found to be ∼1000 Ω m at the five locations in the Pampa La Bola area. The values at the three locations in the Llano de Chajnantor area were much higher, exceeding 3500 Ω m. This difference probably reflects differences in water content in the upper soil layer due to local topography and drainage. The depths of the upper layer of broken rock found at these sites are of order a few meters, and are consistent with depths found from borehole cores obtained near each location.

1 Introduction

Soil resistivity is a basic parameter necessary for the design of effective grounding and lightning prevention/protection systems. In addition, resistivity profiling can yield information on characteristics (including depth) of different layers in the subsurface. The resistivity of rocks or soils is in general a complicated function of their porosity, permeability, ionic content of pore fluids, and mineralization. In most rock materials, the porosity and the ionic content of the pore fluid are more important in governing resistivity than the conductivity of the constituent mineral grains. In situations where the porous rocks lie well above the water table and the fraction of the pores filled with fluid is negligibly small, mineralization starts to contribute. Igneous rocks tend to have higher resistivity than sediments. Lavas and tuffs have very high values ranging from 10^2 to 5×10^4 Ω m and from 2×10^3 to 10^5 Ω m, respectively, whereas unconsolidated wet clay is known to have resistivity as low as ∼20 Ω m [1]. Given that the soils in the Cerro Chascón area are derived from ignimbrites, and that they are located in one of the world's driest deserts, the soil resistivity in the Cerro Chascón science preserve area is expected to be very high.

Soil resistivity is usually measured in the field. During resistivity surveys, current is injected into the ground through a pair of current electrodes, and the potential difference is measured between a pair of potential electrodes. The current and potential electrodes are generally arranged in a linear array. Common arrays include the Schlumberger array, the Wenner array, the dipole-dipole array, and the pole-pole array. The choice of array depends on the nature of the study and the limits of the instrument. For instance, in some situations the power of the instrument is insufficient for successful Schlumberger measurements, in which case the Wenner configuration may be used. Dipole-dipole with small instruments is reported to be successful only for very shallow imaging at archaeological sites.

Two different methods have been widely applied: resistivity mapping and resistivity sounding. In resistivity mapping, the electrode spacing is fixed, and measurements are taken at successive intervals to map the spatial distribution of apparent soil resistivity. These types of measurements are used to map faults, map lateral extent of conductive contaminant plumes, locate voids, map heavy metal soil contamination, delineate disposal areas, explore for sand and gravel, and map archaeological sites.

Measurements of apparent soil resistivity at the surface have also been extensively used as a rapid, non-invasive way to sound the vertical profile of electrical resistivity. The apparent surface resistivity is the bulk average resistivity of all soils and rock influencing the flow of current. It is calculated by dividing the measured potential difference by the input current, and multiplying by a geometric factor (specific to the array being used and electrode spacing). In resistivity soundings, the distance between the current electrodes or the distance between the current and potential dipoles is expanded in a regular manner between readings, thus yielding information on the electrical properties of soils from deeper and deeper depths. The apparent resistivity is virtually the same as the resistivity of the surface material when the electrode spacing is very small compared to the thickness of the surface layer, whereas it approaches the resistivity of the lower material when the electrode spacing is large compared with the thickness of the surface layer because the portion of the current confined to the surface layer becomes negligible. Models of the variation of resistivity with deppth can be obtained in a more quantitative way using model curves or forward and inverse modeling computer programs. One obvious advantage of this method is that the electrodes are located near the surface, thus eliminating the need for costly boreholes for site investigation. These types of measurements are used to characterize subsurface hydrogeology (to, e.g., determine depth to bedrock/overburden thickness, depth to groundwater, map stratigraphy, map clay aquitards, or map salt-water intrusion), map vertical extent of certain types of soil and groundwater contamination, and estimate landfill thickness.

Here we report results of resistivity sounding of eight locations distributed in the Cerro Chascón science preserve area, using the Wenner electrode configuration with electrode spacings up to 81 m.

2 Theoretical Background

Application of the surface resistivity method requires that an electrical current be injected into the ground by surface electrodes. A series of probes at the surface are used to inject low-frequency currents into the ground and to measure local variations in surface potential differences. Suppose a point current source is used to inject a current I_0 into the surface of a homogeneous soil with specific resistance ρ. The electric potential V_p at distance r_0 is expressed as

$$V_p = -\int_{\infty}^{r_0} \frac{\rho I_0}{2\pi r^2} dr = \frac{\rho I_0}{2\pi r_0} \quad . \tag{1}$$

The equipotential surfaces are hemispherical for a homogeneous soil.

Next consider the specific configuration illustrated in Figure 1 (the Wenner configuration). The potential at P_1 is $(\rho I_0/2\pi)/(1/a - 1/2a)$, whereas the potential at P_2 is $(\rho I_0/2\pi)/(1/2a - 1/a)$. The resulting potential field (voltage) is measured at the surface by a voltmeter between electrodes. The voltage between P_1 and P_2 would be $V_0 = \rho I_0/2\pi a$ and the resistivity of the subsurface material ρ can be calculated by knowing the electrode configuration, the electrode spacing a, the applied current I_0, and the measured voltage V_0 as

$$\rho = 2\pi a(V_0/I_0) \quad . \tag{2}$$

In the actual measurements care must be taken to avoid the effects of ground resistance of the electrodes on the results. These represent isolated single-boundary measurements of quite

large equipotential surfaces which are hemispherical for a homogeneous soil, but which will be distorted considerably by the presence of regions of variable electrical conductivity or buried objects.

For a two-layered soil with a surface layer of resistivity ρ_1 and thickness d_1 overlying an infinitely thick substratum of resistivity ρ_2, the measured apparent soil resistivity ρ will change in a different way as a function of the probe spacing. In this case the electric potential V_p at distance r_0 is expressed as

$$V_p = \frac{\rho I_0}{2\pi}\left[\frac{1}{r_0} + 2\sum_{n=1}^{\infty}\frac{k^n}{(r_0^2 + 4n^2{d_1}^2)^{1/2}}\right] \quad , \tag{3}$$

where k is the resistivity reflectivity for dc currents: $k \equiv (\rho_2 - \rho_1)/(\rho_2 + \rho_1)$. In the Wenner configuration, the voltage between P_1 and P_2 is

$$V_0 = \frac{\rho_1 I_0}{2\pi a}\left[1 + 4\sum_{n=1}^{\infty}\frac{k^n}{(1 + 4n^2{d_1}^2/a^2)^{1/2}} - 2\sum_{n=1}^{\infty}\frac{k^n}{(1 + n^2{d_1}^2/a^2)^{1/2}}\right] \quad , \tag{4}$$

and then the apparent soil resistivity ρ for a two-layered soil can be compared with that calculated by knowing the geometry of the electrode positions, the electrode spacing a, the applied current I_0, and the measured voltage V_0 as

$$\frac{\rho}{\rho_1} = 1 + 4\sum_{n=1}^{\infty}\frac{k^n}{(1 + 4n^2{d_1}^2/a^2)^{1/2}} - 2\sum_{n=1}^{\infty}\frac{k^n}{(1 + n^2{d_1}^2/a^2)^{1/2}} \quad , \tag{5}$$

where again $k \equiv (\rho_2 - \rho_1)/(\rho_2 + \rho_1)$. Results for a multi-layered soil can be analyzed in the same manner.

The interpretation of resistivity soundings in terms of depths and true electrical resistivities of horizontally layered units requires the use of forward filters or sounding inversion. Consequently, more than one depth-resistivity multilayer model may fit the same resistivity sounding data. The final interpretation depends partly on the expertise and judgment of the geophysicist, especially taking into account additional information on the site (notably, information from boreholes can restrict the possible solutions).

3 Measurements and Analysis

The measurements were conducted from June 25 to July 3 (local winter) and on September 11 (local spring) of the year 2000 with a Yokogawa Type 3244 surface resistivity instrument. The Wenner electrode configuration was used to obtain the apparent resistivity values. We used five electrodes in each configuration as indicated in Figure 1. Soil resistivity was measured with nine sets of electrode spacings per location to obtain the depth profile of the soil resistivity. The spacings of the probes (a in Figure 1) were selected to be 1.00, 1.73, 3.00, 5.20, 9.00, 15.59, 27.00, 46.77, and 81.00 m to provide uniform sampling on a logarithmic scale. Uniform sampling on a logarithmic scale is better to deduce properties of both upper and lower layers than any other sampling (such as uniform sampling on a linear scale) for given number of spacings. Another merit of this carefully chosen sets of electrode spacings is that we could share the electrodes and save the labor of setting and removing the electrodes by a factor of 2. The depth of each electrode was set at about 20 cm.

We measured eight locations in total, including all six locations where boreholes were previously dug (Pampa La Bola, the ASTE site near the NRO containers, Chajnantor North, Chajnantor South, the Chascón–Chajnantor saddle point, and Chascón East). The other two

locations were the NRO testing site and the NRAO/ESO testing site. These locations, as measured with a navigation GPS, are shown in Figure 2 and tabulated in Table 1.

A commercial software package (RINVERT) was used to construct the resistivity pseudo-sections beneath the line of electrodes.

4 Results and Discussion

4.1 Depth Profile of Soil Resistivity

Figure 3 shows plots of apparent soil resistivity at all the locations as a function of the probe spacing. Data points with arrows pointed upward are lower limits, and those with parentheses have large associated uncertainty.

The apparent values with short probe spacings were used as estimates of the soil resistivity near the surface. These values were found to be $\sim$1000 Ω m at the four positions in the Pampa La Bola area (the ASTE site near NRO containers, the NRO testing site, Pampa La Bola, and Chascón East). The values at the three positions in the Llano de Chajnantor area (Chajnantor North, Chajnantor South, and the NRAO/ESO testing site) were significantly higher and exceeded 3500 Ω m.

Except for the Chajnantor–Chascón saddle point, the soil resistivity seems to approach a global value of $\sim$2000 Ω m, which is typical for massive rocks, as the probe spacing increases (in other words, as we probe to deeper levels). This is consistent with our understanding that at these locations, the surface is covered with broken rocks to a depth of only a few meters, with massive rocks below that upper layer [3].

As we have seen above, the apparent soil resistivity measured as a function of the electrode spacing indicates existence of at least three characteristic layers beneath the locations: the first one with large point-by-point variation, the second one with a global value of $\sim$2000 Ω m, and the last one with much lower resistivity. In order to analyze the data in more quantitative way, we adopted for simplicity three-layer model for the fitting.

Table 2 summarizes the parameters of the best-fit three-layer model of soil resistivity at each location deduced with the RINVERT software. Parameters of equivalently good models are also tabulated. The uncertainty in the fits is high for the three locations in the Llano de Chajnantor area. This is probably due to large intrinsic errors in the individual measurements caused by very high ground resistance of the electrodes. In addition, the parameters of the third layer have large uncertainty in most cases, and so we focus on the fit parameters of the first two layers.

For those locations where boreholes were previously dug, the depth of the upper (broken rock) layer deduced from the resistivity profiles in this study are consistent with those measured from the borehole cores. For instance, the depth of the upper layer was measured to be 2.0 m both at Chajnantor North and Chajnantor South from the borehole cores [3], while it is estimated to be 2.13 and 1.53 m for these two locations in this study. The much deeper upper layers at the Chajnantor–Chascón saddle point and Chascón East were also reproduced.

4.2 Why is the Surface Resistivity at the Llano de Chajnantor Locations So High?

There is a significant difference in the surface values of the soil resistivity between the Llano de Chajnantor and Pampa La Bola locations. Another important fact is that the resistivity of the upper layers at the Llano de Chajnantor locations is higher than that of bedrock, whereas the upper layers at the Pampa La Bola locations have lower values than that of the bedrock. Why do the Llano de Chajnantor locations have such high surface values of soil resistivity?

Through previous geotechnical studies of the entire region [3,4], we have learned that the material of the subsurface layer is almost identical throughout the area except for the Chajnantor–Chascón saddle point. The difference between the Pampa La Bola and Llano de Chajnantor locations may then be understood as a probable difference in the water content of the weathered rocks near the surface, i.e., the upper layers of the Llano de Chajnantor locations are much drier than the upper layers of the Pampa La Bola locations. A recent study of the local weather [5] indicates that it is not likely that precipitation falls preferably in the Pampa La Bola area, so that should not be the cause of higher water content in that location. From a topographical point of view, all of the measured points in the Llano de Chajnantor area are located on ridges, whereas all of the locations in the Pampa La Bola area are located in very flat regions. We therefore suggest that the soil resistivity near the surface is higher in the Llano de Chajnantor area because the water drainage is more effective in this area, keeping the upper layers very dry. This idea is consistent with the results of underground temperature profiling: low thermal conductivity of the layer near the surface at Llano de Chajnantor [6], and relatively high thermal conductivity of the layer near the surface at Pampa La Bola [7].

4.3 Future Work

It is obviously important to map wider areas along the possible loci of LMSA/ALMA configurations. In this soil resistivity mapping (as opposed to profiling), we recommend a value of the fixed electrode spacing of 2 m – good for probing the resistivity of the upper layer. Measurements should be carried out in a short period of time so that the measured values are not severely affected by possible diurnal variations and other possible longer time variations (due to rain/snow etc.).

At the probable locations for the LMSA/ALMA compact configuration, the time variation of surface resistivity should be monitored with sets of fixed electrodes. The surface resistivity during summer, when the lightning hazard is highest, is of highest priority. Independent information on the freezing–melting cycle as well as the water drainage should be obtained.

We thank Bryan Butler and Atsushi Yashima for critical review and comments that significantly improved this work, and Hiroya Andoh, Tetsuo Hasegawa, Tamio Hashimoto, Hirokazu Honda, Yoshiaki Moriguchi, Toshikazu Ohnishi, Tomohiko Sekiguchi, Toshiaki Takano, Nobuharu Ukita, and Satoshi Yamamoto, who helped the work at 5000 m altitude.

References

[1] Telford, W. M., Geldart, L. P., & Sheriff, R. E. 1990, "Applied Geophysics (Second Edition)," (Cambridge: Cambridge University Press)

[2] NRAO 1999, "Topographical Map of CONICYT Science Preserve"

[3] NRO-NRAO 2000, "Geotechnical Study, Chajnantor Site, II Region," LMSA Memo 2000-04

[4] NRAO 1998, "Geotechnical Feasibility Report (Rev. A), MMA Project"

[5] Sakamoto, S., Handa, K., Kohno, K., Nakai, N., Otárola, A., Radford, S. J. E., Butler, B., & Bronfman, L. 2000, "Comparison of Meteorological Data at the Pampa La Bola and Llano de Chajnantor Sites," LMSA Memo 2000-08 (also ALMA Memo 322)

[6] Snyder, L. A., Radford, S. J. E., & Holdaway, M. A. 2000, "Underground Temperature Fluctuations and Water Drainage at Chajnantor," ALMA Memo 314

[7] Sakamoto, S. 2000, "Thermal Properties of Subsurface Layer at Pampa La Bola, Chile," LMSA Memo, in preparation

Table 1: GPS Positions (UTM/UPS WGS84) of Measurement Locations.

ID	East	North	Altitude	Description
Pampa La Bola	0633650	7460200	4800 m	Candidate ALMA array center. Borehole site #1.
NRO	0633170	7459680	4800 m	NRO testing site.
ASTE	0632940	7459040	4800 m	ASTE candidate site. Borehole site #2.
Saddle point	0631250	7455850	4900 m	Chascón-Chajnantor saddle point. Borehole site #5.
Chajnantor N.	0627410	7454050	5030 m	Candidate ALMA array center. Borehole site #3.
NRAO/ESO	0627770	7453770	5050 m	NRAO/ESO testing site.
Chajnantor S.	0627610	7452850	5030 m	Candidate ALMA array center. Borehole site #4.
Chascón E.	0637710	7457280	4630 m	North-east of Cerro Chascón. Borehole site #6.

Table 2: Best-Fit Three-Layer Models.

ID	Layer	Depth	Thickness d_n (m)			Resistivity ρ_n (Ω m)		
	n	(m)	best	min	max	best	min	max
Pampa La Bola	1	0.00	0.66	0.40	0.72	1628	942	1789
	2	0.66	32.58	31.51	37.17	2832	2652	2957
	3	33.25	∞			1429	1339	1547
NRO	1	0.00	3.63	3.43	3.86	1180	1117	1223
	2	3.63	37.77	32.35	41.43	1753	1657	1858
	3	41.40	∞			1248	1174	1315
ASTE	1	0.00	3.52	3.10	3.73	687	662	708
	2	3.52	43.93	38.78	48.12	3015	2780	3311
	3	47.45	∞			144	132	156
Saddle point	1	0.00	8.68	6.98	9.45	1119	918	1227
	2	8.68	5.07	1.34	6.88	4335	3345	15121
	3	13.75	∞			313	282	340
Chajnantor N.	1	0.00	2.13	1.89	3.42	4759	2960	5716
	2	2.13	22.60	20.69	30.79	1956	1360	2113
	3	24.73	∞			191	178	208
NRAO/ESO	1	0.00	1.24	0.95	1.64	3579	2945	4354
	2	1.24	319.95	302.35	343.30	1986	1829	2134
	3	321.19	∞			44	41	45
Chajnantor S.	1	0.00	1.53	0.34	1.72	5119	4700	25479
	2	1.53	12.25	8.32	20.74	1371	810	2120
	3	13.78	∞			839	757	891
Chascón E.	1	0.00	7.58	6.11	8.87	829	716	910
	2	7.58	36.58	28.12	46.71	2054	1689	2485
	3	44.16	∞			851	777	927

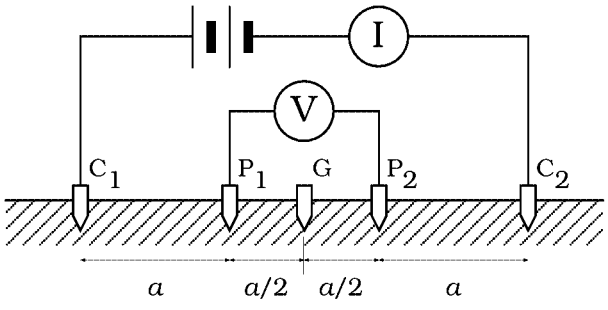

Figure 1: The Wenner electrode configuration. Current is injected into the ground through a pair of current electrodes (C_1 and C_2), and the potential difference is measured between a pair of potential electrodes (P_1 and P_2). The input voltage is not dc as indicated in this figure but square-wave ac to avoid effects of natural current and polarization near the current electrodes.

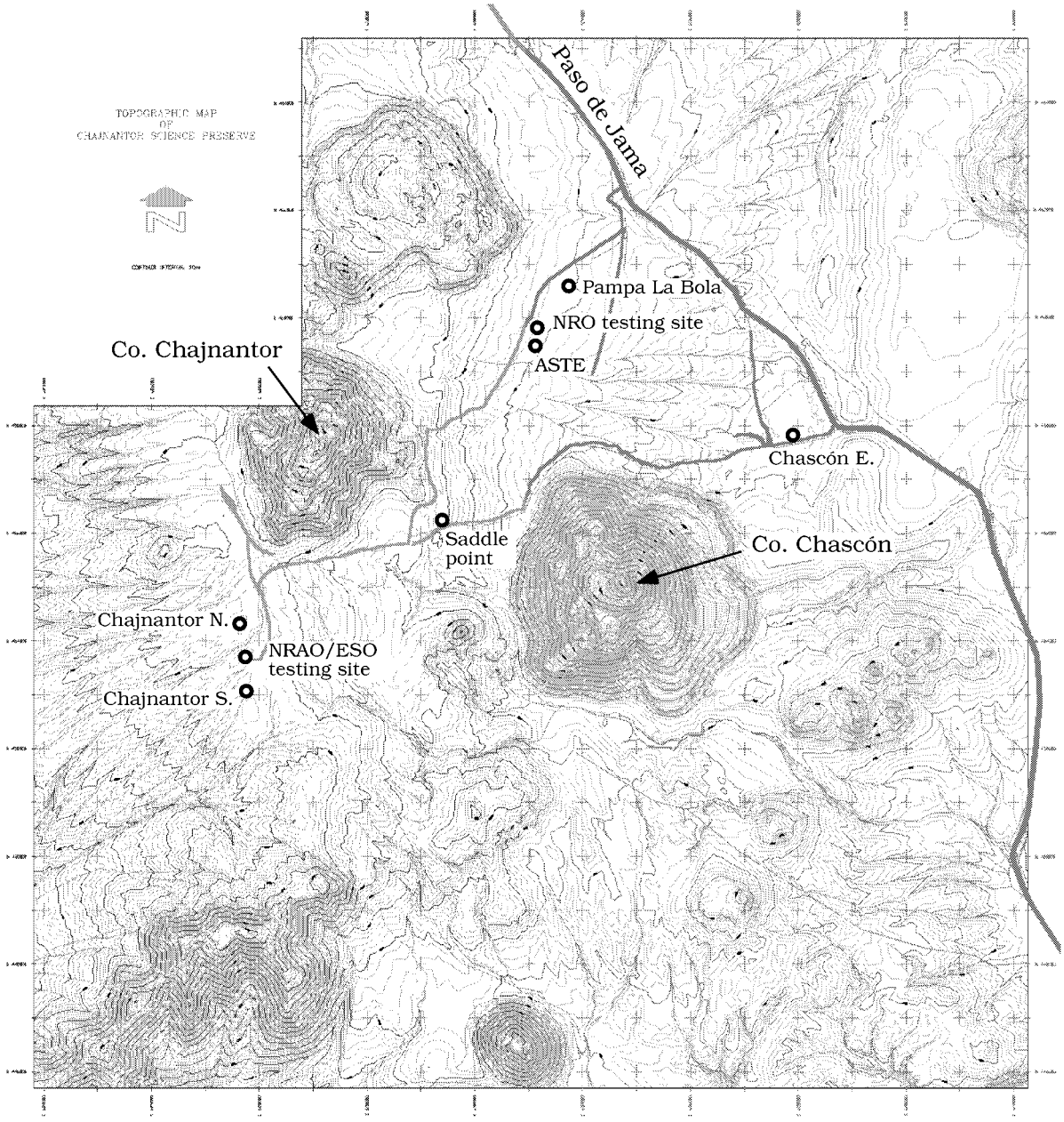

Figure 2: Positions of the measurement locations overlaid on the topographic map of the Cerro Chascón science preserve area [2]. The absolute coordinates may contain errors up to a few 100 m. Ticks are spaced by 1 km. Contour spacing is 10 m with thick contours every 50 m. The international highway (Paso de Jama) and some of the unpaved roads are marked with thick lines. The volcanic peak in the middle of this area is Cerro Chascón. Cerro Chajnantor is to the WNW of Cerro Chascón.

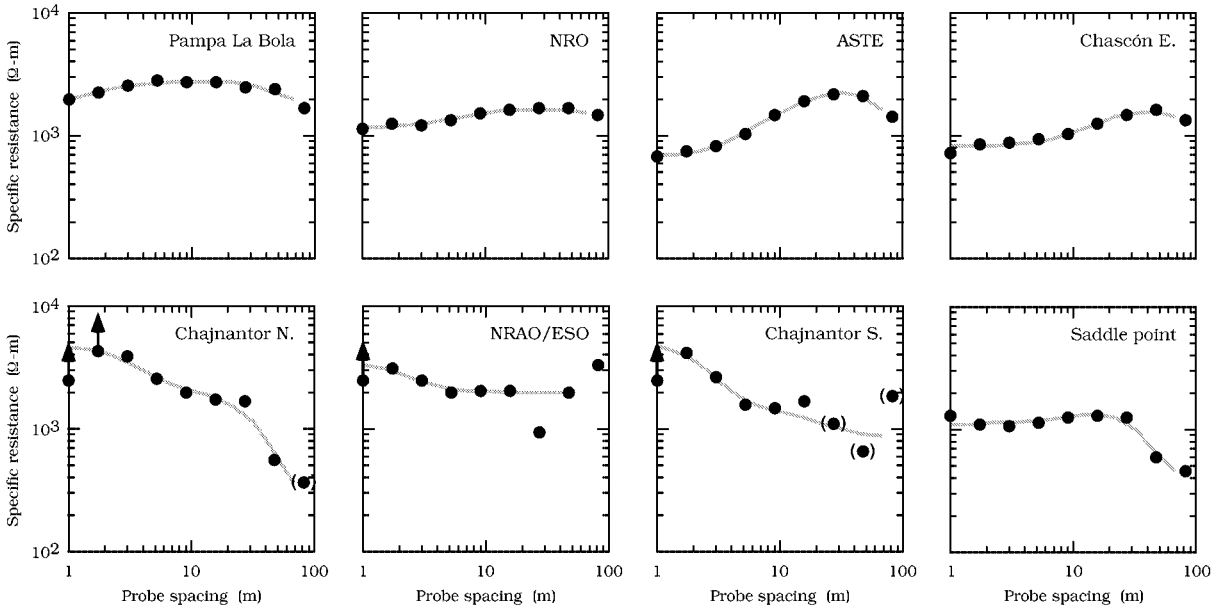

Figure 3: Apparent soil resistivity at eight locations in the Cerro Chascón science preserve area as a function of the probe spacing. Data points with arrows pointed upward are lower limits, and those with parentheses have large associated uncertainty. Theoretical curves of the best-fit three-layers models are also shown.